IEEE Access
Multidisciplinary | Rapid Review | Open Access Journal

Received September 16, 2019, accepted October 19, 2019, date of publication October 28, 2019,
date of current version November 13, 2019.

Digital Object Identifier 10.1109/ACCESS.2019.2949747

On-Line Gait Adjustment for Humanoid Robot Robust Walking Based on Divergence Component of Motion

SHENG DONG[1], ZHAOHUI YUAN[1], XIAOJUN YU[1], JIANRUI ZHANG[1], MUHAMMAD TARIQ SADIQ[1,2], AND FULI ZHANG[1]

[1]School of Automation, Northwestern Polytechnical University, Xi'an 710072, China
[2]Department of Electrical Engineering, The University of Lahore, Lahore 54000, Pakistan

Corresponding authors: Zhaohui Yuan (yuanzhh@nwpu.edu.cn) and Xiaojun Yu (xjyu@nwpu.edu.cn)

This work was supported in part by the National Natural Science Foundation of China under Grant 61705184 and Grant 51875477, in part by the Natural Science Basic Research Plan in Shaanxi Province of China under Grant 2018JQ6014, in part by the Fundamental Research Funds for the Central Universities under Grant G2018KY0308, in part by the China Postdoctoral Science Foundation under Grant 2018M641013, in part by the Training Project of Postgraduate Innovation Competition Team in Northwestern Polytechnical University, in part by the Doctoral Fund Project of Longdong University under Grant XYBY1901, and in part by the Higher Education Innovative Ability Enhancement Project of Gansu Province under Grant 2019A-113.

ABSTRACT As the first step for biped robots to enter the human life, robust walking is a difficult problem to be solved owing to the various algorithms and practical engineering issues being involved. This paper studies the robust walking problem for humanoid robots by using the divergence component of motion (DCM) method based on linear inverted pendulum model. Firstly, we implement a DCM trajectory planning method to simplify the planning process. It calculates the DCM trajectories under the requirements of walking speed and initial state of the system. Then, a DCM feedback controller with anti-disturbance ability is proposed to realize the tracking control of the planned trajectory. Finally, the optimization method and DCM feedback control are integrated into a hybrid optimization controller, which takes into account the step adjustment and the step duration adjustment of the robot. Simulation results demonstrates that the technique can act naturally stable inside an enormous scope of effect unsettling influences, the maximum recoverable impact of a humanoid robots with a mass of 70Kg can reach 85Ns, which is much better than the 20Ns of the existing model-based prediction control method.

INDEX TERMS Biped robot, humanoid robot, divergence component of motion (DCM), gait generation, adaptive step duration.

I. INTRODUTCION

Leg movement is the basic function for robots to complete various advanced task, and it influences the dynamic balance of humanoid robots. Due to the complexities of its hybrid dynamics, however, the unidirectional constraints on the contact forces, the high dimensionality as well as the nonlinearity of robot general dynamics, the leg movement of robots is broadly respected to be a troublesome issue [1]. In literature, a common method to tackle such a problem is to use the overall dynamics of the robot to optimize the walking gait. However, the calculation of the dynamic equations requires tons of computational assets. Moreover, due to the possible non-convexity of the optimization problem, the global minimum may not be guaranteed. Therefore, it is useful to simplify the overall dynamics process to a set of linear equations for real-time gait generation, and the linear inverted pendulum model (LIPM) [2] or its variant three mass linear inverted pendulum model (3M-LIPM) [3] have been applied in designing complex biped walking controllers. Specifically, based on a predefined zero-torque point (ZMP) [4] trajectory, Kajita *et al.* [5] proposed a ZMP predictive control to generate a center of mass (CoM) trajectory, while Wieber [6] improved the performance of this method under relatively severe thrust by recalculating the foothold in the Model Predictive Control (MPC) [7] framework. These predictions and optimization-based trajectory planning methods use quadratic to process motion details. Since the linear model is simple, the problem

The associate editor coordinating the review of this manuscript and approving it for publication was Zhonglai Wang.

of linear quadratic programming (QP) was introduced. However, there are a lot of convenient tools for solving the application specific QP problems, most of them still suffer from the computational complexity and the limited anti-disturbance capabilities due to the limitations of the pre-requisites for predictive use, such as fixed stride distances or fixed stride times.

Furthermore, these real-time gait generation methods [8]–[11] based on MPC optimization directly generate the trajectory of CoM and the center of pressure (CoP), and the stable and unstable parts of LIPM are all involved in the calculation, resulting in a large amount of optimization calculation. So Takaneka *et al.* [12] decomposed the LIPM into a stable part (inertial link) and an unstable part, then introduced an intermediate variable - the DCM. In the trajectories planning calculation, only the unstable link is considered, and the DCM trajectory is generated according to the predefined footprint, CoM tracks DCM based on natural dynamics, which simplifies the gait generation algorithm. Prior to [12], DCM was used by Hof [13], in the name of the extrapolation quality center to explain human walking characteristics. Pratt *et al.* [14] named DCM as a capture point (CP) and used it as a break point that the robot should step on. Englsberger *et al.* [15] proposed a feedback control method that controls CoP in real-time to operate the DCM to track the planned trajectory. The controller responds very quickly to disturbances, but for a fully driven robot with a finite-size foot, the movement of the CoP is limited (the supporting polygon is ranged), so the disturbance suppression capability of the robot is also limited. While for a point-foot robots, it is impossible to operate CoP.

Therefore, the DCM-based small-scale optimization control method is exceptionally appealing. For the stability problem of gait, one can get inspirations from the human beings. For example, when people are disturbed by small external disturbances, they can maintain stability by changing the position of CoP in the soles of the feet. While when people are largely disturbed, step adjustment is a more important tool for maintaining stability. This is because the next landing position in a relatively large area can be selected in the step. Even for point-footed with limited joint motion, there is a larger step adaptive region than the contact point in a very limited environment. Hence, Herdt *et al.* [16] and Diedam *et al.* [8] used predictive control to include the step distance into the optimization objective function, making the footsteps variable to generate both CoM and CoP trajectories while obeying the CoP constraints. Results showed that the generated walking mode is robust to unsettling influences, even with high level target tasks such as desired step position or walking speed. It is worth noting that all those methods have not considered the influences of step duration to the change of landing speed. In practice, however, the step-distance adjustment contributes only to disturbance energy consumption, the step duration adjustment could help adjust the robot foot movement speed. Since the CoM trajectory is a nonlinear function of both the time and the initial conditions,

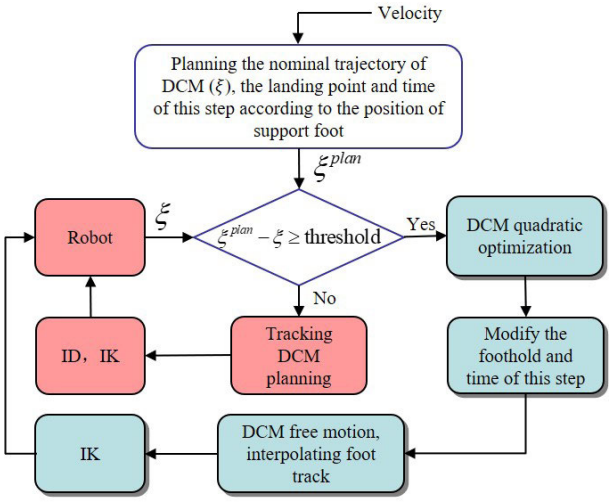

FIGURE 1. Optimal control structure of walking machine.

in order to deal with non-linear optimization problems, many algorithms have been proposed in the literature [17]–[21]. Kryczka [22] and Aftab [9] proposed a solution that utilizes a nonlinear optimization technique to modify both footstep positions and step-timing in order to maintain dynamic stability during the robot walking process. Specifically, Aftab introduced a simple model of the mechanical cost in the objective function by penalizing the acceleration of the swing foot, while the acceleration can't anyway exceed a given maximum value. Kryczka rewrote the optimization objective to be a non-linear function of the optimization variables. Although satisfactory results have been achieved, the nonlinear optimization process introduced high computational costs, and cannot guarantee convergence to the minimum either.

With the influences of step-timing to the change of landing speed taken into account, this paper studies the on-line gait adjustment of humanoid robots. When there is a disturbance, DCM would have a large deviation from the planned trajectory, and thus, an optimized method is used to find the settled footing and stride time. The disturbed landing point and stride time are used as optimization variables to minimize the error between the stride distance and the nominal value, as well as the stride time and the nominal value. The mechanical structural constraints and stability conditions are used as hard constraints for small-scale optimization calculations without DCM tracking control. If there is no disturbance or the DCM deviation caused by disturbance is small, the trajectory of the DCM is then planned according to the target speed, and the real-time tracking control is performed to enhance the robustness of the gait. Fig. 1 shows the control flow of the whole gait adjustment process.

The main contributions of this study could be summarized as follows. First, we proposed a DCM trajectory planning method, which can quickly calculate the DCM trajectory according to the set speed and initial state, and does not need to pre-set the foothold sequence like Englsberger [23]. Second, according to the planned DCM trajectory, a feedback

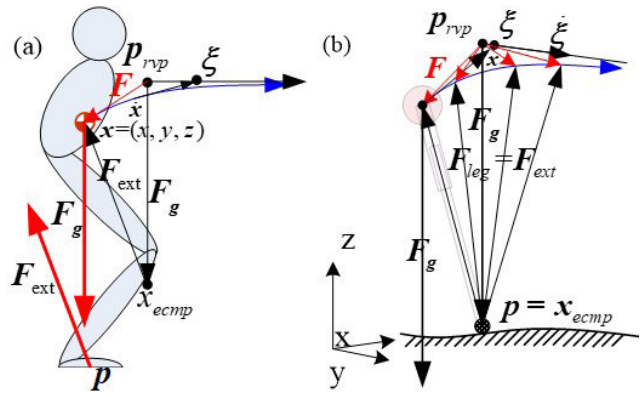

FIGURE 2. Force analysis of biped robot. (a) General force conditions of the robots, ξ is the DCM, p_{rvp} is the starting point of gravity. (b) Equivalent sketch.

controller is designed, which can compensate for a certain range of disturbances by moving CoP during the walking process of the robot. Finally, in the case of large disturbances, we propose a hybrid controller based optimization. The controller can take both step timing and step distance into account, and actively change the preceding DCM planning trajectory.

The remainder of this paper is organized as follows. Section II reviews the background of DCM and presents the DCM trajectory planning method with target walking speed. In Section III, the DCM-based step distance and stride time optimization adjustment methods are studied, and then, the feedback control is combined to form a hybrid optimization controller. Simulation results and discussions are described in Section IV, while Section V concludes the paper.

II. THE GENERATION AND CONTROL OF STANDARD CONTINUOUS DCM TRAJECTORIES

A. BACKGROUND

The actual biped is subjected to general forces in three-dimensional space as shown in Fig. 2. The CoM is only affected by gravitational force $\boldsymbol{F_g}$ and external forces $\boldsymbol{F_{ext}}$. There are multiple $\boldsymbol{F_{ext}}$ to maintain the stability of the robot, and the direction of external force on the legs is not necessarily along the CoP (point $\boldsymbol{p}$) to the CoM (point $\boldsymbol{x} = (x, y, z)$). The resultant force on the CoM is,

$$\boldsymbol{F} = \boldsymbol{F_g} + \boldsymbol{F_{ext}} = m\ddot{\boldsymbol{x}} \tag{1}$$

and

$$\boldsymbol{F_{ext}} = K(\boldsymbol{x} - \boldsymbol{x_{ecmp}}) \tag{2}$$

where $\boldsymbol{x_{ecmp}}$ is the virtual intersection of $\boldsymbol{F_g}$ and $\boldsymbol{F_{ext}}$ in space, and K is the coefficient. In order to facilitate gait planning, we choose a special $\boldsymbol{F_{ext}}$. When there is no disturbance, the $\boldsymbol{F_{ext}}$ always points to the CoM along the CoP, and the abstract equivalent of Fig. 2(a) is Fig. 2(b). Currently, $\boldsymbol{x_{ecmp}}$ and $\boldsymbol{p}$ coincide, $\boldsymbol{x_{ecmp}} = \boldsymbol{p} = [p_x\ p_y\ p_z]^T$.

For LIPM, Eq. (1) is then rewritten as follows:

$$F = \underbrace{\begin{bmatrix} 0 \\ 0 \\ -mg \end{bmatrix}}_{F_g} + \underbrace{\frac{mg}{z - p_z}(x - p)}_{F_{ext}} = \begin{bmatrix} m\omega^2 (x - p_x) \\ m\omega^2 (x - p_y) \\ 0 \end{bmatrix} \tag{3}$$

where $\boldsymbol{x} = [x\ y\ z]^T$ is the CoM coordinates, $\boldsymbol{p} = [p_x\ p_y\ p_z = 0]^T$, and let

$$\frac{mg}{z - p_z} = m\omega^2 = \frac{m}{b^2} \tag{4}$$

here, b is the time constant of LIPM dynamics, ω is the natural frequency of LIPM. $\boldsymbol{F_g}$ and $\boldsymbol{F_{ext}}$ cancel each other vertically in order to make $\ddot{z} = 0$ and keep $z - p_z$ constant. When the LIPM is used for biped walking control, the ZMP is assumed to be equivalent to the fulcrum of the inverted pendulum. In real robots, due to the imprecision of the model, p usually deviates from the target point in the operation. If we plan a set of feasible p in advance and adjust attitude in real time, feedback tracking is a more feasible method. Stephens and Atkeson [24] proposed an MPC gait adjustment method, which changed the p-point to achieve the goal of push recovery.

If $z(t) - p_z(t) = \Delta z = const$ can be guaranteed in 3D space, and $p_z \neq 0$, $z \neq const$, the DCM planning and control in the x, y direction can be applied to the z direction. That is to say

$$\boldsymbol{\xi} = \boldsymbol{x} + \boldsymbol{b}\dot{\boldsymbol{x}} \tag{5}$$

Here, ξ is the DCM, In addition, there is

$$\dot{\boldsymbol{\xi}} = \frac{\mathbf{1}}{\boldsymbol{b}}(\boldsymbol{\xi} - \boldsymbol{p}) \tag{6}$$

where $\boldsymbol{\xi} = [\xi_x\ \xi_y\ \xi_z]^T$, $\dot{\boldsymbol{x}} = [\dot{x}\ \dot{y}\ \dot{z}]^T$ is the CoM speed. The DCM is defined as a point located at a certain distance in front of the current moving direction of the CoM. Then solving Eq. (6) can get,

$$\boldsymbol{\xi}\ (\boldsymbol{t}) = (\boldsymbol{\xi_0} - \boldsymbol{p})\, \boldsymbol{e^{\omega t}} + \boldsymbol{p} \tag{7}$$

after the end of the step timing T,

$$\boldsymbol{\xi}\ (\boldsymbol{T}) = \boldsymbol{\xi_T} = (\boldsymbol{\xi_0} - \boldsymbol{p})\, \boldsymbol{e^{\omega T}} + \boldsymbol{p} \tag{8}$$

In particular, if the CoM does not move in the z direction, the average speed during walking is not changed artificially, T does not change, and in the x-y plane.

$$\left\| \boldsymbol{\xi}_{T,k} - \boldsymbol{p}_{k+1} \right\| = \left\| \boldsymbol{\xi}_{0,k} - \boldsymbol{p}_k \right\| = \boldsymbol{d} \tag{9}$$

can be obtained for the k-th step. As shown in Fig. 3, $\boldsymbol{\xi}_{T,k} = \boldsymbol{\xi}_{0,k+1}$

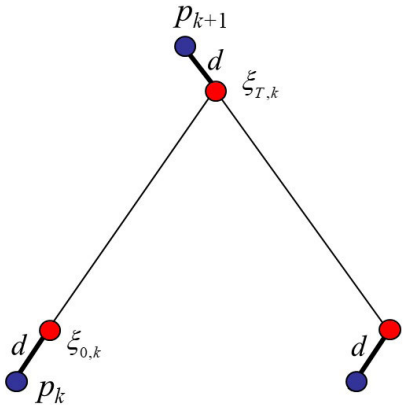

FIGURE 3. The relationship between DCM and ZMP (p-point) in the planning process.

B. GENERATION AND CONTROL OF DCM TRAJECTORY

Based on the above, the generation and control method of DCM trajectory is deduced, assuming that: the upper body of the robot does not rotate, and the change of angular momentum is 0.

It is known that the support foot p_k of the k-th step and the target speed v_x, v_y, the maximum distance X_{max}, Y_{max} and the minimum step distance X_{min}, Y_{min} of each step in the x, y direction according to the mechanical structure are also known, and stepping time is bounded. then

$$\frac{X_{\min}}{|v_x|} \leq T_{nom} \leq \frac{X_{\max}}{|v_x|} \tag{10}$$

$$\frac{Y_{\min}}{|v_y|} \leq T_{nom} \leq \frac{Y_{\max}}{|v_y|} \tag{11}$$

$$T_{\min} \leq T_{nom} \leq T_{\max} \tag{12}$$

It should be noted that Eq. (10) and Eq. (11) are effective for non-zero velocity. In the case where the velocity in one of the directions is zero, the inequality in that direction is ignored. In order to make all the above inequalities tenable

$$T_{low} \leq T_{nom} \leq T_{upper} \tag{13}$$

where $T_{low} = \max\left(\frac{X_{\min}}{|v_x|}, \frac{Y_{\min}}{|v_y|}, T_{\min}\right)$, $T_{upper} = \min\left(\frac{X_{\max}}{|v_x|}, \frac{Y_{\max}}{|v_y|}, T_{\max}\right)$, then

$$T_{nom} = \frac{T_{low} + T_{upper}}{2} \tag{14}$$

$$\begin{cases} X_{nom} = v_x T_{nom} \\ Y_{nom} = v_y T_{nom} \end{cases} \tag{15}$$

$$\begin{cases} p_{k+1,x} = p_{k,x} + X_{nom} \\ p_{k+1,y} = p_{k,y} + Y_{nom} + (-1)^{n+1} hip \end{cases} \tag{16}$$

where n is used to distinguish which foot is the supporting foot. $n = 1$ means the right foot, $n = 2$ means the left foot. *hip* indicates the natural width of the two feet when the robot legs are perpendicular to the ground. From Eq. (7), Eq. (9) and Eq. (16) get,

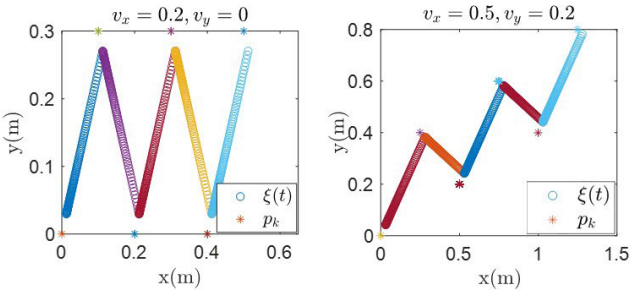

FIGURE 4. The DCM planning trajectory under two kinds of walking conditions.

$$d_{x,nom} = X_{nom} \Big/ \left(e^{\omega T_{nom}} - 1\right) \tag{17}$$

$$d_{y,nom} = (-1)^{(n+1)} \left(hip \Big/ \left(1 + e^{\omega T_{nom}}\right)\right) - Y_{nom} \Big/ \left(1 - e^{\omega T_{nom}}\right) \tag{18}$$

So,

$$\boldsymbol{\xi}_{0,k} = \left(p_{k,x} + d_{x,nom}, p_{k,y} + d_{y,nom}\right) \tag{19}$$

Finally, the DCM planning trajectory of the current step is

$$\begin{cases} \xi_{k,x}^{plan}(t) = d_{x,nom} e^{\omega t} + p_{k,x} \\ \xi_{k,y}^{plan}(t) = d_{y,nom} e^{\omega t} + p_{k,y} \quad (0 \leq t \leq T_{nom}) \end{cases} \tag{20}$$

The Fig. 4 shows the DCM planning trajectory in two walking states. By inputting the speed, the planning algorithm automatically finds the appropriate foothold and step time. The DCM can adjust the trajectory automatically by changing the walking speed.

In order to make the DCM tracking the plan, we can design the following controller,

$$\dot{\boldsymbol{\xi}}(t) = \dot{\boldsymbol{\xi}}^{plan}(t) - K_f(\boldsymbol{\xi}(t) - \boldsymbol{\xi}^{plan}(t)) \tag{21}$$

In this way, the real-time tracking of the DCM is guaranteed by controlling the change of the actual value of the DCM. Where K_f is the coefficient. Combined with Eq. (5), the closed-loop state space equation can be written as,

$$\begin{bmatrix} \dot{\boldsymbol{x}} \\ \dot{\boldsymbol{\xi}} \end{bmatrix} = \begin{bmatrix} -1/b & 1/b \\ 0 & -K_f \end{bmatrix} \begin{bmatrix} \boldsymbol{x} \\ \boldsymbol{\xi} \end{bmatrix} + \begin{bmatrix} 0 & 0 \\ K_f & 1 \end{bmatrix} \begin{bmatrix} \boldsymbol{\xi}^{plan} \\ \dot{\boldsymbol{\xi}}^{plan} \end{bmatrix} \tag{22}$$

The eigenvalues of this closed loop are $-1/b$ and $-K_f$, so the system is globally stable as long as $K_f > 0$ and $b > 0$, then $\boldsymbol{\xi}(t)$ gradually converges to $\boldsymbol{\xi}^{plan}(t)$. And by the Eq. (6), it can be deduced that the purpose of changing $\dot{\boldsymbol{\xi}}(t)$ can be achieved by changing the support point $\boldsymbol{p}$.

$$\boldsymbol{p_c}(t) = \boldsymbol{\xi}(t) - b\dot{\boldsymbol{\xi}}^{plan}(t) + K_f b(\boldsymbol{\xi}(t) - \boldsymbol{\xi}^{plan}(t)) \tag{23}$$

Because of

$$\dot{\boldsymbol{\xi}}^{plan}(t) = \frac{1}{b}\left(\boldsymbol{\xi}^{plan}(t) - \boldsymbol{p}^{plan}\right) \tag{24}$$

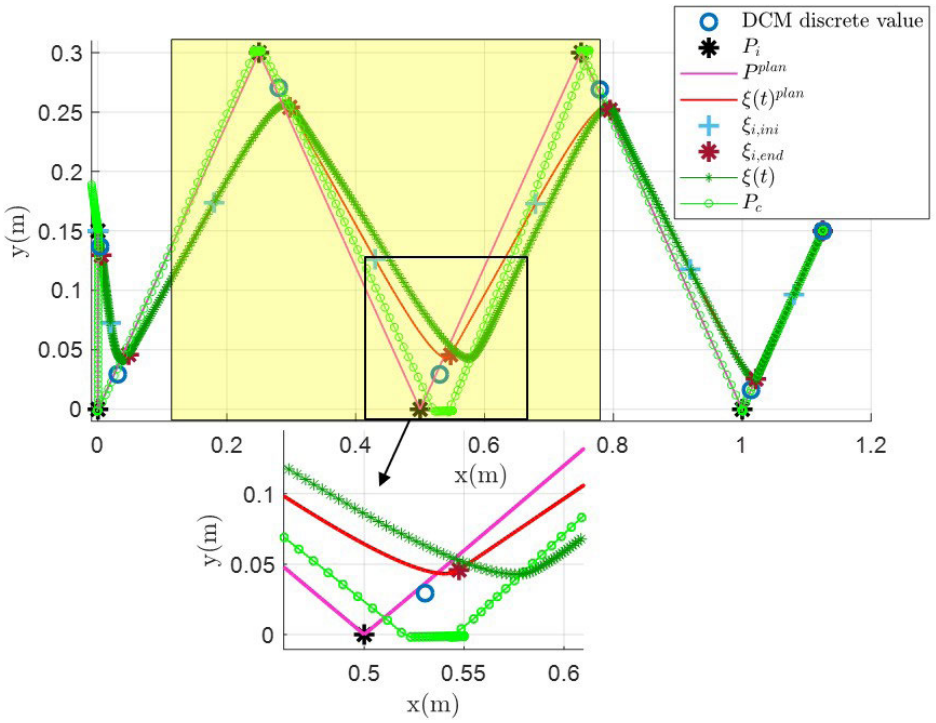

FIGURE 5. Modification of planning trajectory by feedback control. The 40N force is applied in the positive direction of x-axis from 0.5s and lasts 0.8s.

we get

$$\boldsymbol{p_c}(t) = \boldsymbol{p}^{plan} + \left(1 + K_f b\right)\left(\boldsymbol{\xi}(t) - \boldsymbol{\xi}^{plan}(t)\right) \tag{25}$$

It use the real-time DCM feedback values $\boldsymbol{\xi}(t)$ and the planning values $\boldsymbol{\xi}^{plan}(t)$ to change $\boldsymbol{p}^{plan}$, $\boldsymbol{\xi}(t)$ will gradually converge to $\boldsymbol{\xi}^{plan}(t)$, and the K_f determines the convergence speed.

C. THE ANALYSIS OF CONTROLLER PERFORMANCE

In the previous section, we proposed the DCM trajectory controller, which can maintain robustness in the presence of model errors or external disturbances. Fig. 5 shows the trajectory tracking of LIPM (with continuous double support stage [15]) under external x-direction disturbance, without in Y direction. Between $\xi_{i,ini}$ and $\xi_{i,end}$ is the double support in the i-th step. The red and pink are the planned ξ^{plan} and p^{plan} respectively. The external force makes the actual value deviate from the planning. The control curve of the point p is shown as p_c. By partial enlargement, it can be seen that the support point p (or ZMP/CoP) is constantly adjusted within a certain range. The real DCM gradually converges to $\xi^{plan}(t)$ after the disturbance is removed, without divergence.

However, the cost of DCM non diverging is that the location of the ZMP/CoP needs to be adjusted continuously. It can be inferred that if the disturbance is strong, the adjustment range of the ZMP/CoP will inevitably exceed the supporting polygon, causing the actual robot to fall. Therefore, the closed-loop controller designed has limited anti-disturbance capability. For disturbances recoverable by moving ZMP/CoP and compensating for the inaccuracy of LIPM, the controller has a good practical effect. But if we want to further improve the stability of the system, it is necessary to adopt the step adjustment method used by the human.

III. ADAPTIVE STEP BASED ON DCM

Next, we find an optimization method that satisfies the constraints and dynamically adjusts the LIPM's stride distance and step duration. In each control cycle, an optimization solution is performed using the actual feedback of the DCM in order to make the dx, dy, stride distance and stride time as close as possible to the nominal value.

A. OBJECTIVE FUNCTION

By solving the (6), we can get

$$\xi_{T,k} = \left(\xi\left(t\right) - p_k\right) e^{\omega(T-t)} + p_k, \quad 0 \le t \le T \tag{26}$$

Because of

$$p_{k+1} = \left(\xi\left(t\right) - p_k\right) e^{\omega(T-t)} + p_k - d, \quad 0 \le t \le T \tag{27}$$

So let

$$\Delta p = p_{k+1} - p_k = \left(\xi\left(t\right) - p_k\right) e^{\omega(T-t)} - d, \quad 0 \le t \le T \tag{28}$$

where Δp is the step distance, its component in the x direction is X, and the component in the y direction is Y, We can take

the objective function as

$$J(t) = \frac{a_1}{2}\|X(t) - X_{nom}\| + \frac{a_2}{2}\|Y(t) - Y_{nom}\| + \frac{a_3}{2}\|\tau(t) - \tau_{nom}\| + \frac{a_4}{2}\|d_x(t) - d_{x,nom}\| + \frac{a_5}{2}\|d_y(t) - d_{y,nom}\| \quad (29)$$

where $X(t)$, $Y(t)$ is the optimal step distance in the x, y direction calculated at time t, $d_x(t)$, $d_y(t)$ is the offset of DCM. And

$$\tau_{nom} = e^{\omega T_{nom}} \quad (30)$$

$$\tau(t) = e^{\omega T(t)} \quad (31)$$

The planned values in the previous section are able to meet the input speed requirements. In the case of external disturbances, the speed deviates from the expected value. The stride distance also deviates from the plan. It is worth noting that d_x, d_y should not deviate from $d_{x,nom}, d_{y,nom}$, because they determines the stability of the system. Therefore, it is necessary to impose greater weight on these two items to ensure $d = d_{nom}$, and then return to planning through one step adjustment. However, for larger disturbances, $d = d_{nom}$ may not be guaranteed. This will require multiple steps to converge the speed to the desired value.

B. CONSTRAINTS

In order to enable the system to travel at a set speed while meeting the physical and mechanical constraints, and to ensure stability, it is necessary to impose constraints on the above objective function.

Inequality constraint

$$\begin{aligned} X_{\min} \le X(t) &\le X_{\max} \\ Y_{\min} \le Y(t) &\le Y_{\max} \\ e^{\omega T_{\min}} \le \tau(t) &\le e^{\omega T_{\max}} \\ 0 \le d_x(t) &\le \Delta d_x \\ 0 \le |d_y|(t) &\le \Delta d_y \end{aligned} \quad (32)$$

where Δd_x and Δd_y is the maximum offset of d in the x, y direction. And $\tau(t) = e^{\omega T(t)}$. In particular, it is also necessary to set $\tau(t) > e^{\omega t}$, which is

$$T(t) > t \quad (33)$$

It shows that the step timing has not yet reached at t-moment, and the walkers have time to adjust.

Equality constraint

The optimization variables need to satisfy Eq. (27) at all times in the control process, eliminating '(t)', and further obtaining,

$$\begin{cases} X = (\xi_x(t) - p_{k,x})\, e^{-\omega t}\tau - d_x \\ Y + (-1)^{n+1} hip = (\xi_y(t) - p_{k,y})\, e^{-\omega t}\tau - d_y \end{cases} \quad (34)$$

In summary, the optimization process is transformed to satisfy constrained inequalities (30), (31) and equality (32) to minimize the objective function $J(t)$.

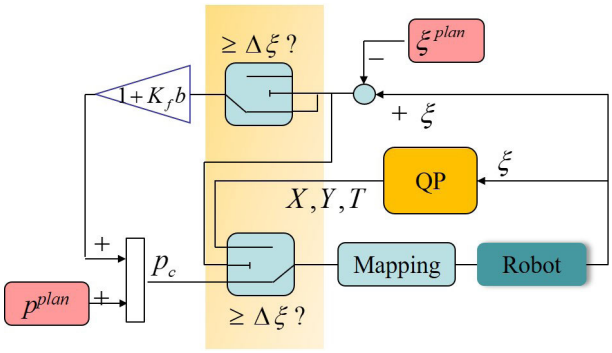

FIGURE 6. Structure diagram of hybrid controller.

C. HYBRID OPTIMAL CONTROL STRUCTURE

In Sec. 2, planning-based CoP adjustment strategy is found by using $\xi(t)$ and $\xi^{plan}(t)$. In Sec. 3.1 and 3.2, a step adjustment strategy without planning is found for larger disturbances. In this way, in the case of undisturbed, the feedback tracking control can be used to compensate the error caused by the inaccuracy of the model, and the planning can be accurately tracked. The small disturbance also has certain robustness. If the DCM deviation from the planning caused by disturbance exceeds the threshold, that is, $\|\xi^{plan} - \xi\| \ge \Delta\xi$. Here $\Delta\xi$ indicates the tolerant deviation between DCM and planning, then cut into optimization, abandon the DCM planning, make DCM move freely. The block diagram of the entire control structure is shown in Fig. 6.

In the closed-loop tracking control, 'Mapping' in Fig. 6 refers to ZMP/CoP controller, inverse dynamics or inverse kinematics, which can be similar to the method in [25] or other ZMP/CoP or torque controller [24], [26]–[28]. In the optimization loop, it refers to the inverse kinematics solution based on X, Y, and T, to find the angle of the joint that acts on each joint. In particular, if DCM is free motion in the optimization loop, the trajectory of the swing foot needs to be generated by cubic or quintic spline interpolation to achieve the desired value after the designated landing point and step timing of the swing foot at the end of a step. Since the next footprint and step timing can be changed during each control cycle, this process should be performed in real time. In fact, the trajectory of the swing foot should be regenerated every control cycle to smoothly connect the desired swing foot state in the previous control cycle to the desired state at the end of the step

IV. RESULTS AND DISCUSSIONS

This section will simulate and analyze the advantages of the proposed hybrid control method for multiple scenarios. Firstly, the effect of DCM feedback tracking control without disturbance (or small disturbance) is simulated to illustrate the necessity of feedback tracking control.

Next, a large external disturbance force is applied to observe the action of the feedback tracking control, which shows the limitation of the feedback tracking control only.

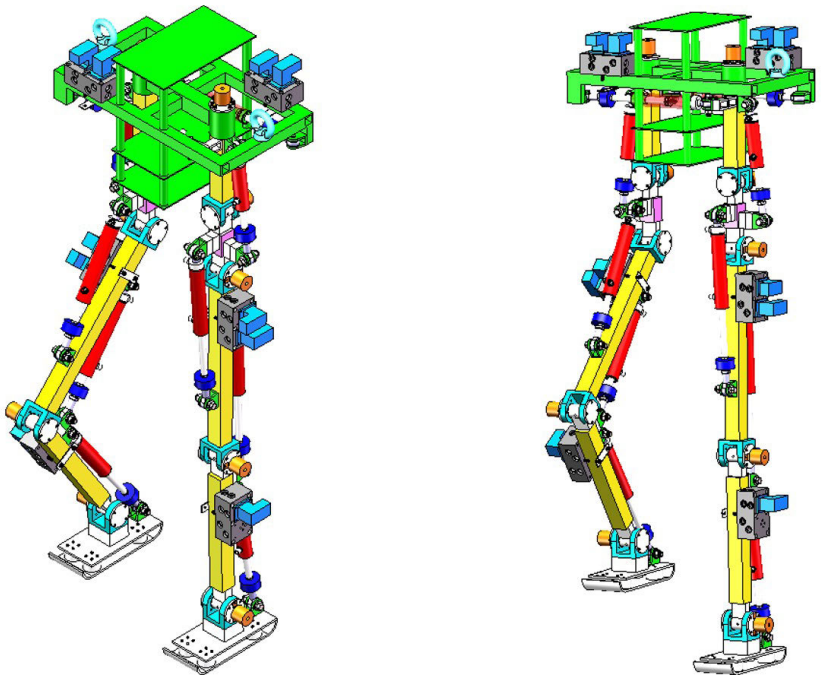

FIGURE 7. The biped robot.

TABLE 1. The description of the robot.

Mass	Leg: 19.5Kg × 2, Trunk: 29Kg
Size	Height: 167cm, Width: 54cm
DoF	Leg: 5 ×2
Actuation	Single ended cylinder(hydr)
Power supply	15 kW hydraulic pump (External) Pressure: 10 MPa (normal), 21 MPa (max)
Onboard sensors	Position, Force, Pressure and ISU
Controllers	32-bit flash memory microcontroller (onboard), PCs (external)
Position sensor	Relative Angle Encoder
Force sensor	Load cell
Signal acquisition system	Control level: 1000 Hz, Servo level: 10 kHz

Finally, a large external disturbance force is applied to the hybrid controller to observe the actual DCM trajectory.

The biped robot used in the simulation is shown in Fig. 7. It is a fully hydraulic-driven robot with a total of 10 degrees of freedom. Each leg has three degrees of freedom (pitch, roll, yaw) on the hip joint, and one pitch DoF on the knee joint and the ankle joint respectively. An angular displacement sensor is installed on each joint. One end of the piston rod of the hydraulic cylinder is equipped with a tension pressure sensor, which can complete the closed-loop of position and force/torque. ISU units are installed on floating base coordinates. The description of the robot is shown in Table 1, and the specific structural parameters are shown in Table 2.

A. DCM FEEDBACK TRACKING CONTROL SIMULATION

This scenario shows the effect of feedback control for small disturbances. The support point p_k is located in the geometric center of the support foot. The robot's walking speed in the x direction is set to be 0.5m/s, and the walking speed in the y direction is 0.0m/s. The ideal ZMP and DCM trajectories with double supports can be found through the research contents of Sec. 2. In fact, even in the case of no disturbance, if we simply open-loop replay programming ZMP (p^{plan}) trajectory, then at least after a period of time, instability will still be observed, since a). there are numerical imprecisions (numerical integration...) and b). the DCM has an unstable dynamic. Furthermore, LIPM will diverge faster if there is disturbance.

The effect of the controller under small disturbances has been shown in Fig. 5 above. For larger disturbances, 142N force is applied in the positive direction of x for 0.2s from 1s. The range of disturbance force in space is shown in the yellow shadow range in Fig. 8. It can be seen that the external force begins in the double support stage, and ZMP drifts rapidly. Especially in the single support stage, ZMP has gone beyond the support polygon. In practice, this is precarious.

TABLE 2. System parameters.

Parameter	Value	Parameter	Value
CoM Height h(m)	0.8	Maximum step distance in x direction X_{max}(m)	0.5
hip(m)	0.01	Minimum step distance in x direction X_{min}(m)	-0.5
Maximum step time T_{max}(s)	0.8	Maximum step distance in y direction Y_{max}(m)	0.3
Minimum step time T_{min}(s)	0.2	Minimum step distance in y direction Y_{min}(m)	-0.2
Length of the foot(m)	0.2	Width of the foot(m)	0.11
Δd_x (m)	0.1	Δd_y (m)	0.05

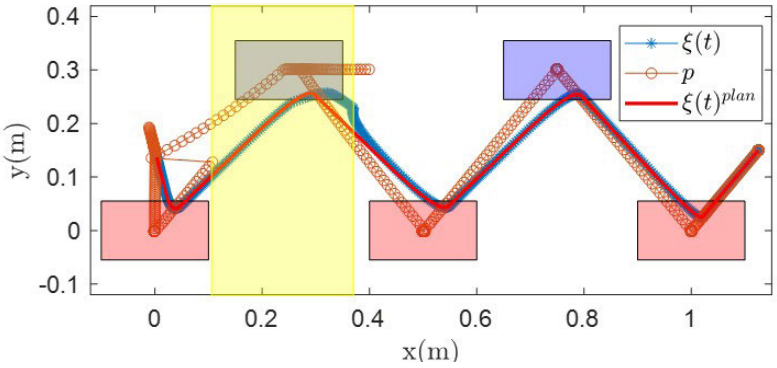

FIGURE 8. The DCM feedback control results for large disturbances.

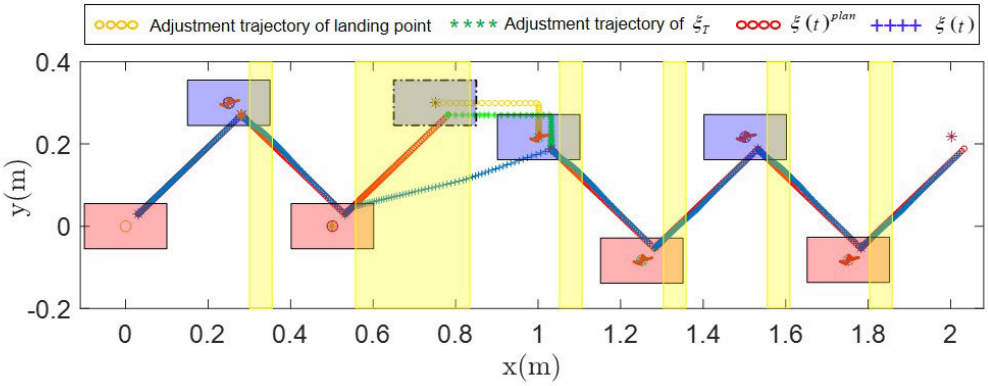

FIGURE 9. Simulation (LIPM) of walking with the nominal speed of 0.5 m/s. The robot is pushed at $t = 1.1$s to the x positive direction with a force $F = 176$ N, during $\Delta t = 0.2$ s. Step location is limited to a rectangular area and the time of stepping is limited with a minimum time (TABLE 2). The system is able to recover from the push by making fast steps on the boundaries of feasible area and continues its walking.

B. HYBRID OPTIMIZATION CONTROLLER SIMULATION

For the above problem, the large disturbance is still applied, and the double support phase is not considered (that is, the ZMP (p^{plan}) trajectory is discrete point), and the hybrid optimization controller is connected. During the third step, an external force of 176N is applied in the positive direction of the x and lasts for 0.2s. It is worth noting that in order to ensure that there is still $d = d_{nom}$ after the end of the step, it is necessary to impose a larger weight on d_x, d_y. Then a fixed small disturbance is applied in the positive direction of x, y during each step, and the spatial disturbance range is shown by the yellow shade in Fig. 9 to observe the action of the hybrid controller.

It can be seen that the footstep of the third step robot has made a large adjustment. At this time, the robot does freely swing because there is no feedback control. A large offset of DCM occurs, but due to the optimization adjustment, the position of the swinging foot of the robot also appeared in a wide range of movements, completing its recapture [29]. After the end of the step, d_x, d_y is still equal to the nominal value, so it can keep on running as arranged. It is only necessary to adjust all the physical quantities back to the plan by one step. The DCM in the x, y direction is shown in Fig. 10. The step time of the third step is significantly shorter, resulting in a fast push-recovery of the robot. Therefore, the impact resistance is improved, and the disturbance impact momentum is 35.2 Ns.

The small disturbance during the period is also controlled by feedback, and it also achieves a good compensation. The movement of ZMP during control is shown by the red curve

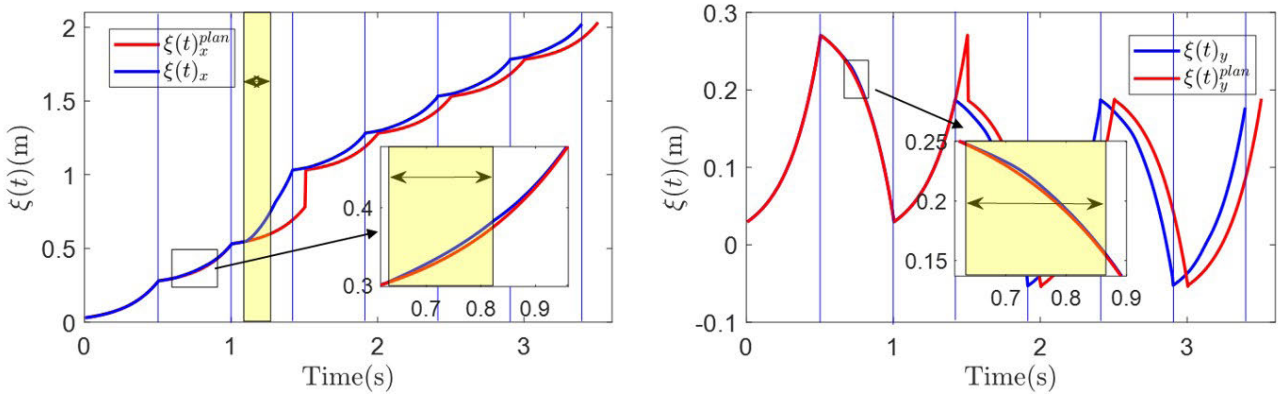

FIGURE 10. The DCM in the x, y direction. The yellow shade in the figure indicates the range of the disturbance.

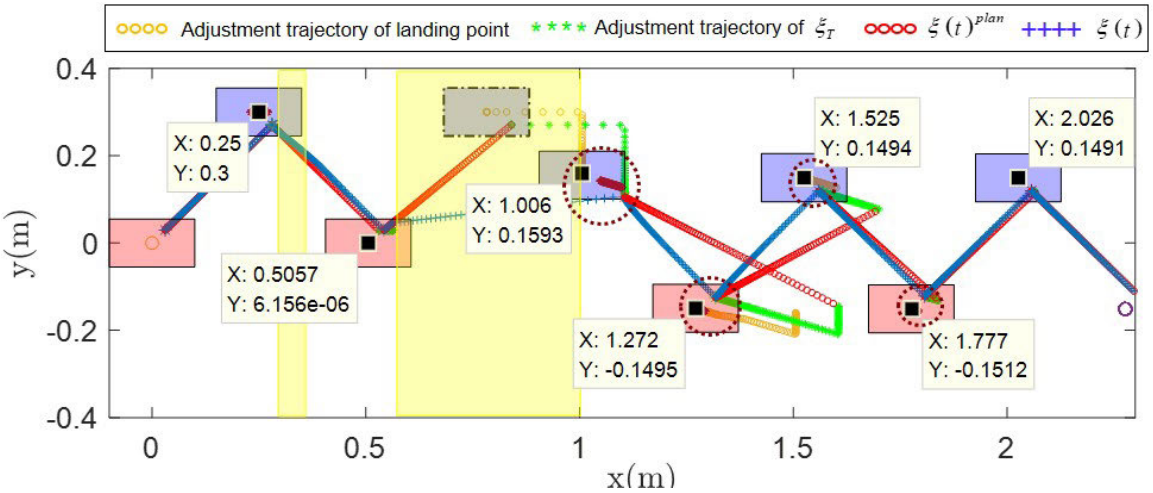

FIGURE 11. Simulation (LIPM) of walking with the nominal speed of $v_x = 0.5$ m/s. The robot is pushed at $t = 1.1$s to the x positive direction with a force $F = 411.6$ N, during $\Delta t = 0.2$ s. The red dashed circle in the figure covers the DCM offset d of the current step, and it gradually returns to d_{nom} with multiple steps. $\xi(t)$ accurate tracking $\xi^{plan}(t)$.

in the footprint of Fig. 9, which only moves in a small range around p_k. By testing the algorithm in one step, the maximum impact in the x direction can withstand 70.56Ns. The maximum y direction can withstand the impact of 58.8Ns, because the mechanical range of motion in the y direction is smaller than the x direction.

Finally, if the disturbance is further increased, the stability requirement may not be met by only one step, and the convex optimization problem won't find a feasible solution. At this time, it is necessary to restore the balance through multiple steps. In the optimization algorithm, it is necessary to reduce the weight coefficient of d_x, d_y, so that they appears larger than the nominal value. Fig. 11 shows the gait of the third step when the disturbance impulse momentum is 82.32Ns in the forward direction of x. In the third step, the robot has the largest step and brings $d > d_{nom}$. The increase of d causes the DCM planning to deviate from the set speed in the fourth step (as shown by the red 'o' curve in the fourth step). Therefore, the plan is invalid. In order to make the robot return to the setting more quickly, d_{nom} is still used for DCM planning (not shown in Fig. 11) during the fourth step, and feedback control is provided. Due to the control effect, $\xi(t)$ gradually returns to the DCM planning using d_{nom}. The change of $\xi(t)$ brings about the decrease of d by optimization, and the stride distance in the x, y direction is gradually closer to X_{nom}, Y_{nom}. After a few steps, d gradually returns to d_{nom}, and the robot continues to walk as set. $\xi(t)$ and the velocity curves during the period are shown in Fig. 12. Through several adjustments, the CoM velocity in the x, y direction is also attributed to the target.

C. DISCUSSIONS

Through the above simulation and comparative analysis, the following points can be obtained:

1. *Robustness*: The proposed method is well matched with the step distance and the step duration, so that the biped can walk robustly, and the anti-disturbing ability is greatly improved compared with the MPC method which

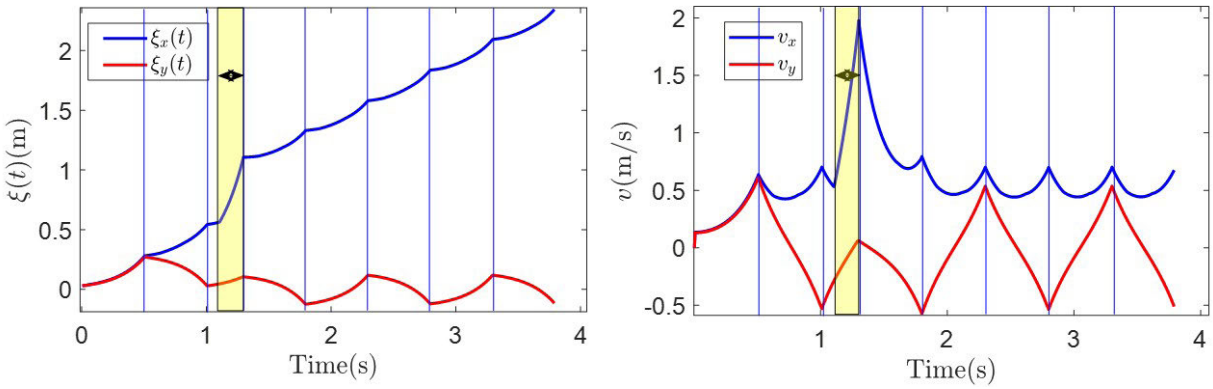

FIGURE 12. The COM velocity in the x, y direction.

only performs stride distance adjustment [10]. In fact, good walking can be achieved without DCM control. Moreover, since the closed loop is cut off during a large disturbance, the robot is free, and the instability caused by the forced movement of ZMP/CoP can be avoided. The closed-loop control with DCM can further compensate for LIPM inaccuracy and numerical integration errors.

2. *Computational efficiency*: The proposed method performs linear quadratic convex optimization. And only the prediction of the current step is performed. This is much simpler than adjusting the stride time in the multi-step prediction horizon in the MPC [22], [28], saving a lot of computing resources. Whether it is an optimization process or a control process, the feedback is only real-time DCM, and the feedback control rate and optimization algorithm can be implemented on any existing platform.

3. *Similarity with people*: The stride produced by this strategy is likewise a comparative technique to human. It is used to resist disturbance, generate larger motion in a shorter time, inhibit DCM/COM divergence. Finally, the speed is attributed to the nominal by multi-step adjustment.

It is worth noting that, since the main focus of this paper is to test the feasibility of the proposed model predictive control algorithm onto the robot, we verified its robustness on flat ground only. When considering some other much more complicated forms of disturbances, like the uneven plane or walking on the slope, however, there may exist various other factors influencing on the performances of the robot. Those factors could impose a huge burden on the performance analysis of biped robots. Therefore, one aspect of our next-step work is to explore and improve the online anti-disturbance performances of the proposed algorithm under complex terrain.

V. CONCLUSION

In this paper we propose a robust gait generation and control method for biped robots. The motion planning of the robot CoM is simplified to the motion planning of DCM, and CoM can track DCM naturally. Combining the feedback control of DCM to compensate for the inaccuracy of LIPM and the numerical integration error, the DCM planning can be applied to the actual robot walking. Then for the push recovery control, QP is applied, and the stride distance, step timing and walking stability factors are used as quadratic objective functions, the physical limits of the robot are written as inequality constraints, and the DCM running rules are used as equality constraints. The step distance and stride time are dynamically adjusted by real-time DCM feedback to achieve the desired DCM offset associated with stability, the gait characteristics are as close as possible to the nominal value. The simulation results show that this method greatly improves the anti-disturbance ability of the biped compared with the DCM feedback control method only. The optimization of step time in the method is linear convex optimization, which solves the nonlinear optimization problem caused by the model predictive control based on CoM motion characteristics to adjust the stride time, and has high computational efficiency.

This study can be regarded as preliminary work for biped robots to enter human life. Our next-step work focuses mainly on the following aspects. First, we are to verify such proposed method on our lab-customized humanoid robot, and then we would like to further extend our method to a three-dimensional space by considering the optimization in z-axis direction. Last but not least, the method could also be extended to uneven ground, within the slope or step environment to mimic the real human living environment to further improve its adaptability.

REFERENCES

[1] A. Pajon, S. Caron, G. De Magistri, S. Miossec, and A. Kheddar, "Walking on gravel with soft soles using linear inverted pendulum tracking and reaction force distribution," in *Proc. IEEE-RAS 17th Int. Conf. Humanoid Robot.*, Nov. 2017, pp. 432–437.

[2] S. Kajita, F. Kanehiro, K. Kaneko, K. Yokoi, and H. Hirukawa, "The 3D linear inverted pendulum mode: A simple modeling for a biped walking pattern generation," in *Proc. IEEE/RSJ Int. Conf. Intell. Robots Syst.*, Oct./Nov. 2001, pp. 239–246.

[3] I.-S. Kim, Y.-J. Han, and Y.-D. Hong, "Stability control for dynamic walking of bipedal robot with real-time capture point trajectory optimization," *J. Intell. Robot. Syst.*, no. 1, pp. 1–17, 2019. [Online]. Available: https://link.springer.com/article/10.1007/s10846-018-0965-7, doi: 10.1007/s10846-018-0965-7.

[4] M. Vukobratović and Y. Stepanenko, "On the stability of anthropomorphic systems," *Math. Biosci.*, vol. 15, pp. 1–37, Oct. 1972.
[5] S. Kajita, F. Kanehiro, K. Kaneko, K. Fujiwara, K. Harada, K. Yokoi, and H. Hirukawa, "Biped walking pattern generation by using preview control of zero-moment point," in *Proc. IEEE Int. Conf. Robot. Autom.*, vol. 2, Sep. 2003, pp. 1620–1626.
[6] P.-B. Wieber, "Trajectory free linear model predictive control for stable walking in the presence of strong perturbations," in *Proc. 6th IEEE-RAS Int. Conf. Humanoid Robots*, Dec. 2006, pp. 137–142.
[7] K. Yu, H. Yang, X. Tan, T. Kawabe, Y. Guo, Q. Liang, Z. Fu, and Z. Zheng, "Model predictive control for hybrid electric vehicle platooning using slope information," *IEEE Trans. Intell. Transp. Syst.*, vol. 17, no. 7, pp. 1894–1909, Jul. 2016.
[8] H. Diedam, D. Dimitrov, P.-B. Wieber, K. Mombaur, and M. Diehl, "Online walking gait generation with adaptive foot positioning through linear model predictive control," in *Proc. IEEE/RSJ Int. Conf. Intell. Robots Syst.*, Sep. 2008, pp. 1121–1126.
[9] Z. Aftab, T. Robert, and P.-B. Wieber, "Ankle, hip and stepping strategies for humanoid balance recovery with a single model predictive control scheme," in *Proc. 12th IEEE-RAS Int. Conf. Humanoid Robots (Humanoids)*, Nov./Dec. 2012, pp. 159–164.
[10] A. Herdt, H. Diedam, P.-B. Wieber, D. Dimitrov, K. Mombaur, and M. Diehl, "Online walking motion generation with automatic footstep placement," *Adv. Robot.*, vol. 24, nos. 5–6, pp. 719–737, 2010.
[11] S. Kim, K. Hirota, T. Nozaki, and T. Murakami, "Human motion analysis and its application to walking stabilization with COG and ZMP," *IEEE Trans. Ind. Informat.*, vol. 14, no. 11, pp. 5178–5186, Nov. 2018.
[12] T. Takenaka, T. Matsumoto, T. Yoshiike, and S. Shirokura, "Real time motion generation and control for biped robot -2nd report: Running gait pattern generation-," in *Proc. IEEE/RSJ Int. Conf. Intell. Robots Syst.*, Oct. 2009, pp. 1092–1099.
[13] A. L. Hof, "The 'extrapolated center of mass' concept suggests a simple control of balance in walking," *Hum. Movement Sci.*, vol. 27, no. 1, pp. 112–125, 2008.
[14] J. Pratt, J. Carff, S. Drakunov, and A. Goswami, "Capture point: A step toward humanoid push recovery," in *Proc. 6th IEEE/RAS Int. Conf. Humanoid Robots*, Dec. 2006, pp. 200–207.
[15] J. Englsberger, T. Koolen, S. Bertrand, J. Pratt, C. Ott, and A. Albu-Schäffer, "Trajectory generation for continuous leg forces during double support and heel-to-toe shift based on divergent component of motion," in *Proc. IEEE/RSJ Int. Conf. Intell. Robots Syst.*, Sep. 2014, pp. 4022–4029.
[16] A. Herdt, N. Perrin, and P.-B. Wieber, "Walking without thinking about it," in *Proc. IEEE/RSJ Int. Conf. Intell. Robots Syst.*, Oct. 2010, pp. 190–195.
[17] C. Shen, L.-H. Zhang, and W. Liu, "A stabilized filter SQP algorithm for nonlinear programming," *J. Global Optim.*, vol. 65, no. 4, pp. 677–708, 2016.
[18] S. Fathi-Hafshejani, H. Mansouri, and M. R. Peyghami, "A large-update primal–dual interior-point algorithm for second-order cone optimization based on a new proximity function," *Optimization*, vol. 65, no. 7, pp. 1477–1496, 2016.
[19] A. Kamandi, K. Amini, and M. Ahookhosh, "An improved adaptive trust-region algorithm," *Optim. Lett.*, vol. 11, no. 3, pp. 555–569, 2017.
[20] Z. Sun, Y. Tian, H. Li, and J. Wang, "A superlinear convergence feasible sequential quadratic programming algorithm for bipedal dynamic walking robot via discrete mechanics and optimal control," *Optim. Control Appl. Methods*, vol. 37, no. 6, pp. 1139–1161, 2016.
[21] Z. B. Sun, Y. Y. Sun, Y. Li, and K. P. Liu, "A new trust region–sequential quadratic programming approach for nonlinear systems based on nonlinear model predictive control," *Eng. Optim.*, vol. 51, no. 6, pp. 1071–1096, 2019.
[22] P. Kryczka, P. Kormushev, N. G. Tsagarakis, and D. G. Caldwell, "Online regeneration of bipedal walking gait pattern optimizing footstep placement and timing," in *Proc. IEEE/RSJ Int. Conf. Intell. Robots Syst.*, Sep./Oct. 2015, pp. 3352–3357.
[23] J. Englsberger, C. Ott, and A. Albu-Schäffer, "Three-dimensional bipedal walking control based on divergent component of motion," *IEEE Trans. Robot.*, vol. 31, no. 2, pp. 355–368, Apr. 2015.
[24] B. J. Stephens and C. G. Atkeson, "Dynamic balance force control for compliant humanoid robots," in *Proc. IEEE/RSJ Int. Conf. Intell. Robots Syst.*, Oct. 2010, pp. 1248–1255.
[25] Y. Choi, D. Kim, Y. Oh, and B. J. You, "Posture/walking control for humanoid robot based on kinematic resolution of CoM jacobian with embedded motion," *IEEE Trans. Robot.*, vol. 23, no. 6, pp. 1285–1293, Dec. 2007.
[26] S. Feng, E. Whitman, X. Xinjilefu, and C. G. Atkeson, "Optimization-based full body control for the DARPA robotics challenge," *J. Field Robot.*, vol. 32, no. 2, pp. 293–312, 2015.
[27] S. Faraji and A. J. Ijspeert, "Singularity-tolerant inverse kinematics for bipedal robots: An efficient use of computational power to reduce energy consumption," *IEEE Robot. Autom. Lett.*, vol. 2, no. 2, pp. 1132–1139, Apr. 2017.
[28] S. Feng, X. Xinjilefu, C. G. Atkeson, and J. Kim, "Robust dynamic walking using online foot step optimization," in *Proc. IEEE/RSJ Int. Conf. Intell. Robots Syst.*, Oct. 2016, pp. 5373–5378.
[29] T. Koolen, T. de Boer, J. Rebula, A. Goswami, and J. Pratt, "Capturability-based analysis and control of legged locomotion, Part 1: Theory and application to three simple gait models," *Int. J. Robot. Res.*, vol. 31, no. 9, pp. 1094–1113, 2012.

SHENG DONG received the B.S. degree from Henan Polytechnic University, in 2011, and the M.S. degree from Northwestern Polytechnical University, Xi'an, China, in 2014, in control engineering, where he is currently pursuing the Ph.D. degree. He was a Software Engineer with the Chinese Academy of Space Technology, responsible for the motion control of large antennas. His research interests include intelligent systems and hydraulic humanoid robot control.

ZHAOHUI YUAN received the B.S., M.S., and Ph.D. degrees in control engineering from Northwestern Polytechnical University, Xi'an, China, in 1984, 1987, and 2005, respectively. He has been with Northwestern Polytechnical University and worked as a Teaching Assistant, a Lecturer, an Associate Professor, and a Professor, since 1987. He has coauthored more than 50 articles in technical journals and conferences. His research interests include high-precision detection instrumentation and system control engineering, hydraulic system control and test, and flow field analysis of the hydraulic systems. He is a Fellow of the Shaanxi Association for Science and Technology.

XIAOJUN YU received the Ph.D. degree from Nanyang Technological University, Singapore, in 2015. From January 2015 to August 2017, he was a Postdoctoral Research Fellow with Nanyang Technological University. He is currently an Associate Professor with Northwestern Polytechnical University, China. His main research interests include high-resolution optical coherence tomography and its imaging applications.

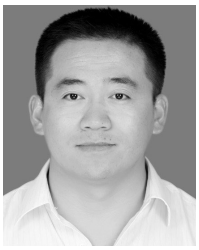

JIANRUI ZHANG received the B.S. and M.S. degrees in mechatronic engineering from Yanshan University, in 2006 and 2009, respectively. He is currently pursuing the Ph.D. degree with Northwestern Polytechnical University, Xi'an, China. He was a Lecturer with the College of Mechanical Engineering, Longdong University. He has published one monograph, published more than ten articles, authorized three patents, and three computer software copyrights. He presided more than two research projects. His research interests include mechatronics and robotics.

MUHAMMAD TARIQ SADIQ received the B.Sc. degree (Hons.) from the Comsats Institute of Information Technology (CIIT), Lahore, Pakistan, in 2009, and the M.Sc. degree in electrical engineering from the Blekinge Institute of Technology (BTH), Sweden, in 2011. He is currently pursuing the Ph.D. degree with Northwestern Polytechnical University, Xi'an, China. He was an Assistant Professor with the Sharif College of Engineering and Technology (SCET), University of Engineering and Technology (UET) Lahore, and a Lecturer with the University of South Asia. He was also the Project Manager at SCET to manage final year student's projects, Patron of the IEEE-SCET Student Branch and a lifetime member of Pakistan Engineering Council (PEC), Islamabad, Pakistan. He is also an Assistant Professor with the Electrical Engineering (EE) Department, The University of Lahore (UOL). His research interest includes biomedical signal analysis and classification.

FULI ZHANG received the B.S. degree in automatic control from the Yanching Institute of Technology, Hebei, China, in 2011, and the M.S. degree in testing technology and automation device from Yanshan University, Hebei, in 2015. He is currently pursuing the Ph.D. degree in control science and engineering with Northwestern Polytechnical University, Xi'an, China, in 2017. His current research interests include robot mechanism design, robot control, and multifield simulation.